Electronic Supplementary Material (ESI) for Nanoscale.

Non-linear Raman scattering intensities in Graphene

Veit Giegold, Lucas Lange, Richard Ciesielski, and Achim Hartschuh*

Department of Chemistry and Center for Nanoscience (CeNS), LMU Munich, Butenandtstr. 5-13, 81377 Munich, Germany

E-mail: achim.hartschuh@lmu.de

1. Comparison of Graphene Raman spectra for cw and pulsed excitation

The detected Raman spectrum of Graphene depends on several experimental parameters including the excitation wavelength, the excitation intensity and the operation mode (cw / pulsed) of the used laser as discussed in the main manuscript. Moreover, the recorded Raman spectrum represents a convolution of the intrinsic Raman lines with the spectrum of the excitation laser and the resolving power of the Raman spectrometer (< 0.5 nm for the present system). Due to the narrow line width of the cw HeNe laser (< 1 GHz) the recorded Raman lines can be expected to directly represent Raman properties of graphene. To compare spectra obtained upon cw- and pulsed excitation, we convoluted the G and 2D Raman lines recorded using cw-excitation from a 633 nm HeNe-laser (green dashed lines in figure S1) with the spectrum of the used pulsed laser source (See inset of figure S1). As reported by Ferrante et al. ultrafast pulsed excitation of graphene leads to additional broadening of the Raman lines from hot carriers for the G and 2D bands.[1] The shown spectra were recorded using $62\,\mu$W excitation power, which corresponds to a maximum carrier

temperature of around 2600 K as derived from the two temperature model discussed below. For this temperature spectral broadening by a factor of 1.35 for the G band and a factor of 2 for the 2D band, respectively, were assumed based on the data in Ref 1. The convoluted spectra (solid black line in figure S1) are in good agreement with the recorded Raman lines for pulsed excitation (dashed blue lines in figure S1) and confirm the comparability of the Raman data obtained by pulsed- and cw-excitation.

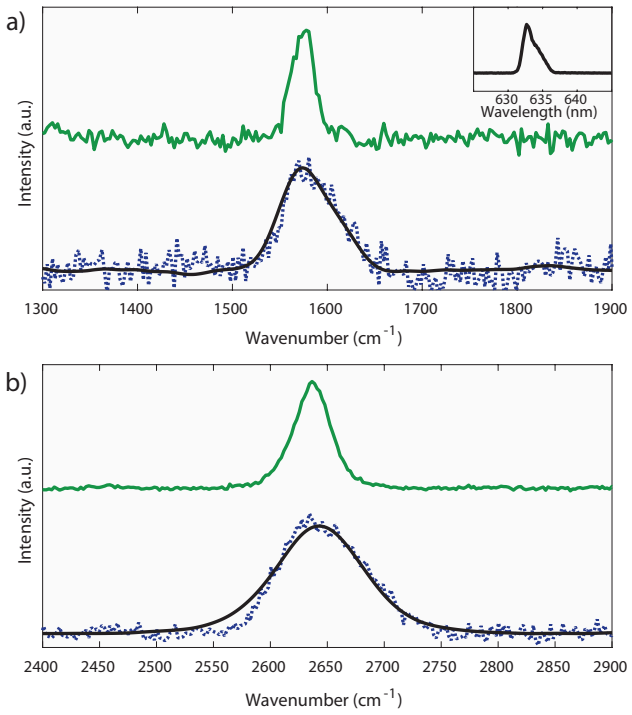

Figure S1: (a) Raman G band recorded with cw-excitation (solid green line) and with pulsed excitation (dashed blue line) at a wavelength of 633 nm. The solid black line is the spectrum obtained after convoluting the Raman spectrum for cw-excitation with the spectrum of the pulsed laser source (small inset). (b) Same as in (a) but for the Raman 2D band. The spectrum obtained after convolution fits the recorded spectrum for pulsed excitation very well.

2. Power dependent Raman measurements for different laser energies

Several measurements series on different locations on the graphene sample were conducted to ensure the observation of an intrinsic effect from graphene. Further experiments using excitation at $594\,\mathrm{nm}$ show that the appearance of the effect is wavelength independent. In Fig. S2 three data sets are shown for excitation at $633\,\mathrm{nm}$ (Fig.S2(a),(b)) and excitation at $594\,\mathrm{nm}$ (Fig.S2(c)). For all experiments a strong increase of the normalized G band and decrease of the 2D band is observed.

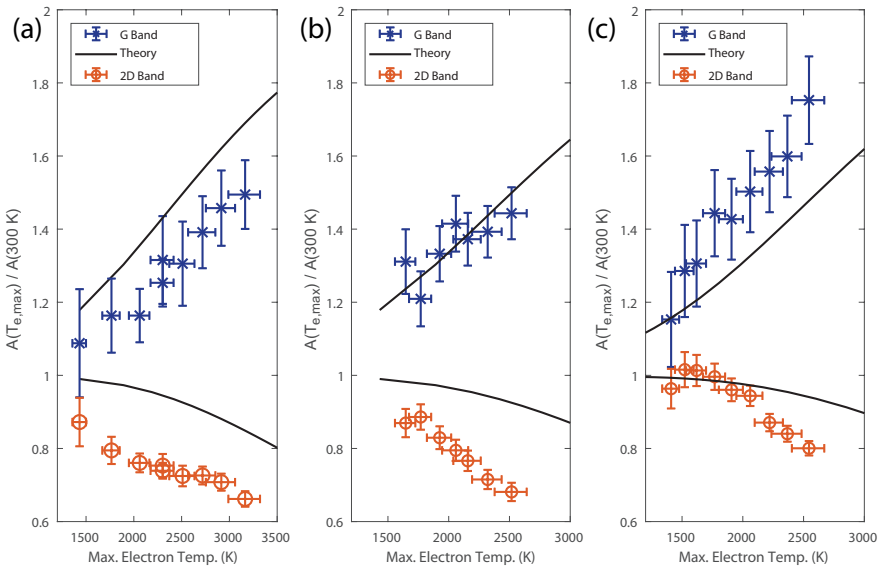

Figure S2: Three data sets from excitation at $633\,\mathrm{nm}$ (a,b) and at $594\,\mathrm{nm}$ (c). The G bands (blue crosses) show a clear decrease for increasing electronic temperature, the 2D bands (orange circles) reduces for increasing electronic temperature, respectively. This behavior is consistent for all data sets.

3. Details on the evaluation of the recorded Raman intensities

3.1 Pulsed excitation at 594 and 633 nm

The following procedure was used to evaluate the spectra recorded for pulsed excitation at 594 and $633\,\mathrm{nm}$. The G- and 2D-Raman signals were first background corrected. The main contributions for the observed background are the fluorescence of the used immersion oil and glass substrate and the thermal emission from graphene. This background contribution was modelled in the spectral range on both sides of the Raman bands using slowly varying model functions. The background corrected Raman signals are shown in figure S3&S4 for $633\,\mathrm{nm}$ excitation, figure S5&S6 for $594\,\mathrm{nm}$ excitation, respectively, as solid blue lines.

Because the best signal to noise ratio is observed for the highest excitation power of each measurement, the G- and 2D-Raman lines of these spectra were chosen to describe the spectra obtained for lower powers for maximum accuracy. To this end, the Raman bands detected for highest power were first fitted by two Gaussian functions to minimize the influence of signal noise. This resulting peak functions were then used to describe all other Raman bands (orange lines in Figs. S3&S4).

For excitation powers below 47 μW we chose three times longer acquisition times to achieve a sufficiently signal to noise ratio. Spectra for 47 μW were recorded for both acquisition times (Figs. S3&S4).

For the data recorded for excitation at 633 nm used in the main manuscript, the amplitudes, areas and linewidths of the 2D and G bands are listed in table 1.

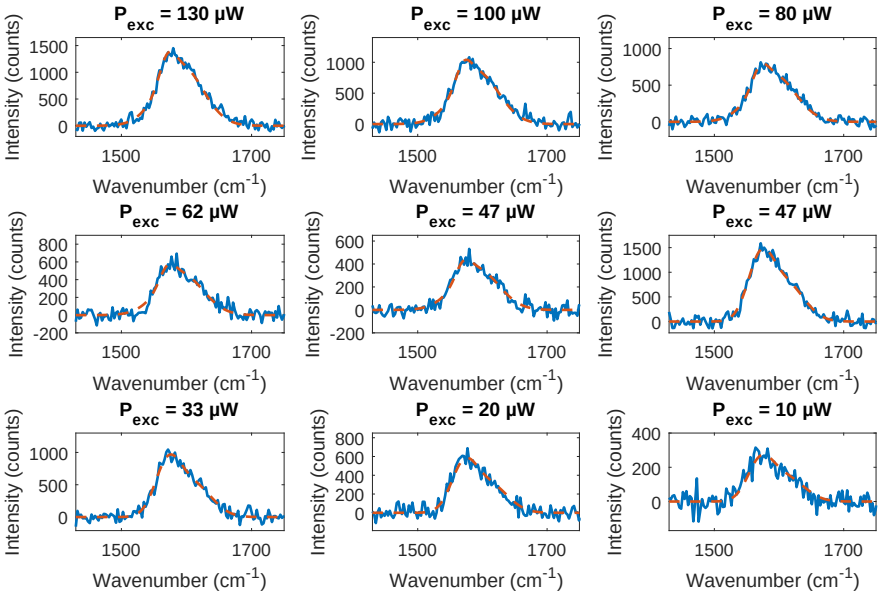

Figure S3: Measured and background corrected G Raman band (blue solid line) for pulsed excitation at 633 nm together with the respective fit functions used to determine the peak area (orange lines).

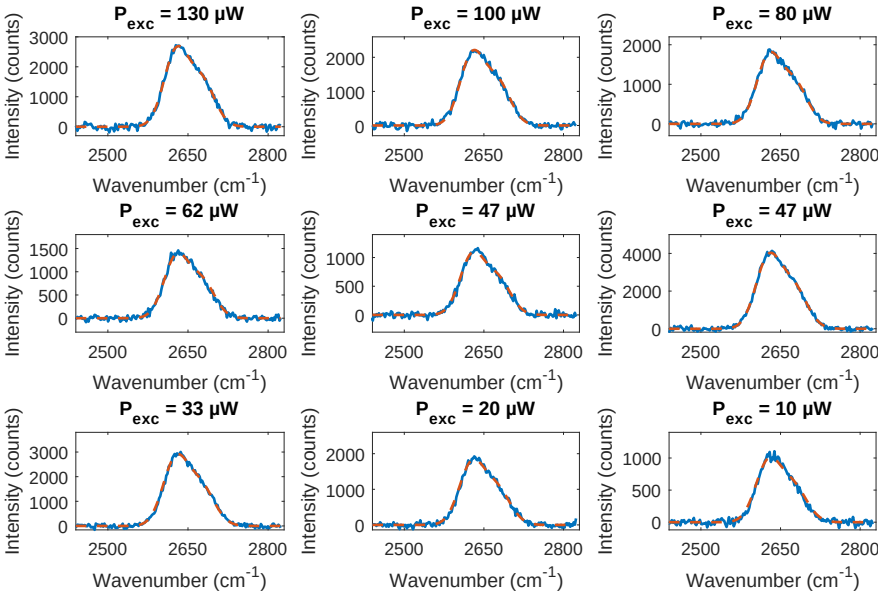

Figure S4: Measured and background corrected 2D Raman band (blue solid line) for pulsed excitation at 633 nm together with the respective fit functions used to determine the peak area (orange lines).

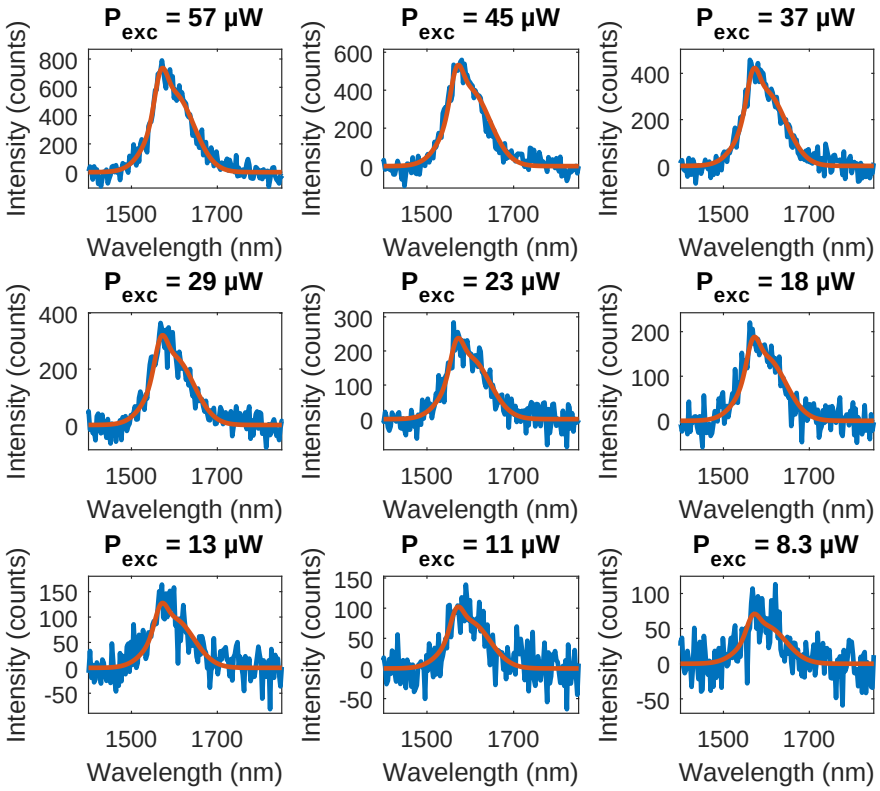

Figure S5: Measured and background corrected G Raman band (blue solid line) for pulsed excitation at 594 nm together with the respective fit functions used to determine the peak area (orange lines).

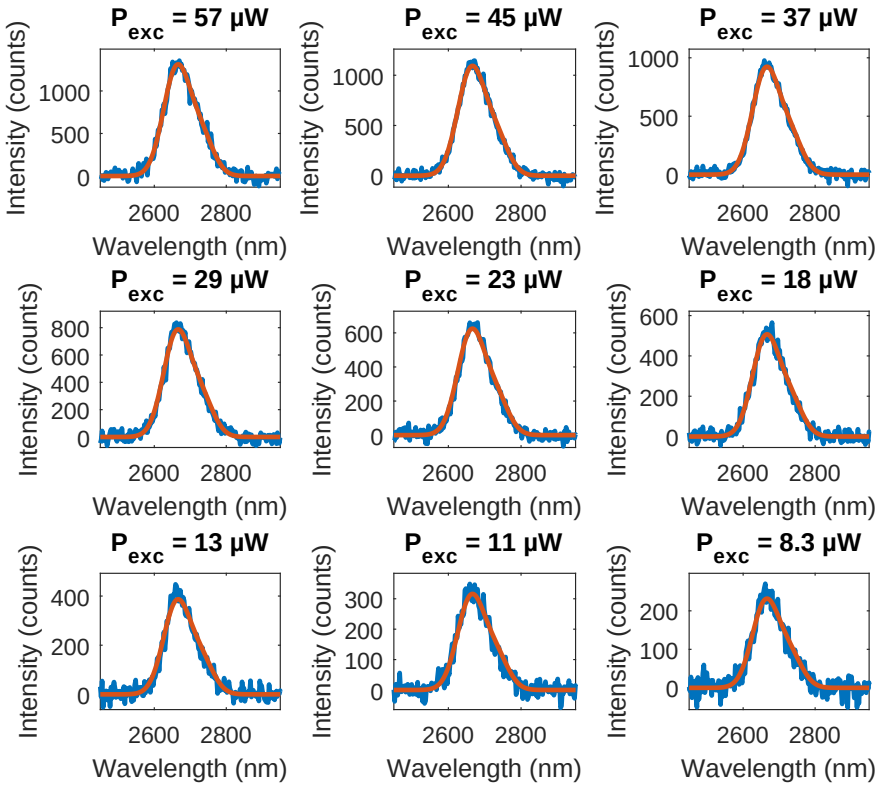

Figure S6: Measured and background corrected 2D Raman band (blue solid line) for pulsed excitation at 594 nm together with the respective fit functions used to determine the peak area (orange lines).

Table 1: Table listing the amplitudes, areas and linewidths of 2D and G bands for pulsed excitation at 633 nm.

2D	Exc. Pow (mW)	Fluence (J/m^2)	Amplitude (a.u.)		Area (a.u.)		FWHM (cm^{-1})	
			Value	±	Value	±	Value	±
	130	3.85	2.69E+03	80	2.31E+05	5.51E+03	84	6
	100	2.96	2.21E+03	80	1.90E+05	4.61E+03	84	6
	80	2.37	1.82E+03	80	1.56E+05	3.78E+03	85	6
	62	1.84	1.41E+03	80	1.21E+05	3.60E+03	82	6
	47	1.39	1.11E+03	80	9.51E+04	3.06E+03	81	6
	47	1.39	4.03E+03	87	3.49E+05	3.53E+02	84	6
	33	0.98	2.91E+03	87	2.52E+05	2.86E+02	83	6
	20	0.59	1.85E+03	87	1.60E+05	2.39E+02	82	6
	10	0.30	1.01E+03	87	8.77E+04	1.80E+02	79	6
G	130	3.85	1.39E+03	77	1.07E+05	6.35E+03	78	6
	100	2.96	1.04E+03	77	8.06E+04	5.37E+03	78	6
	80	2.37	7.94E+02	77	6.16E+04	4.21E+03	79	6
	62	1.84	5.77E+02	77	4.48E+04	4.53E+03	75	6
	47	1.39	4.41E+02	77	3.42E+04	3.41E+03	76	7
	47	1.39	1.49E+03	85	1.11E+05	3.24E+02	74	6
	33	0.98	9.68E+02	85	7.22E+04	2.56E+02	74	6
	20	0.59	5.87E+02	85	4.37E+04	2.19E+02	70	6
	10	0.30	2.74E+02	85	2.04E+04	1.63E+02	74	9

3.2 Raman spectra for different cw excitation intensities

The following procedure was used to evaluate the spectra recorded for cw excitation at 594 and 633 nm. The G- and 2D-Raman signals were first background corrected. The main contributions for the observed background are the fluorescence of the used immersion oil and glass substrate.

The background corrected Raman signals are shown in Figure S7 & S8 for cw excitation at $633\,\mathrm{nm}$ and in Figure S9 & S10 for cw excitation at $594\,\mathrm{nm}$. These Raman signals were integrated and normalized to the used excitation power. Because no spectral variations for cw-excitation for the used powers were observed, these spectra corresponds to an electronic temperature T^e_{max} equal 300 K. Therefore it was used as reference for the Raman band integrals derived from pulsed excitation in figure 2 of the main article.

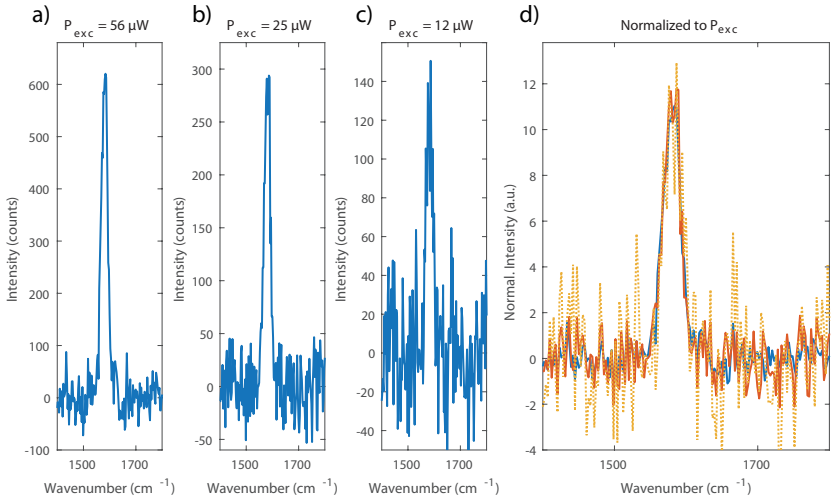

Figure S7: (a),(b) and (c) show the background corrected Raman G band recorded for cw excitation for three different excitation powers at 633 nm. (d) shows the comparison for all four measurements after normalization with the excitation power. The measurement with the lowest intensity is shown as dashed line for better readability.

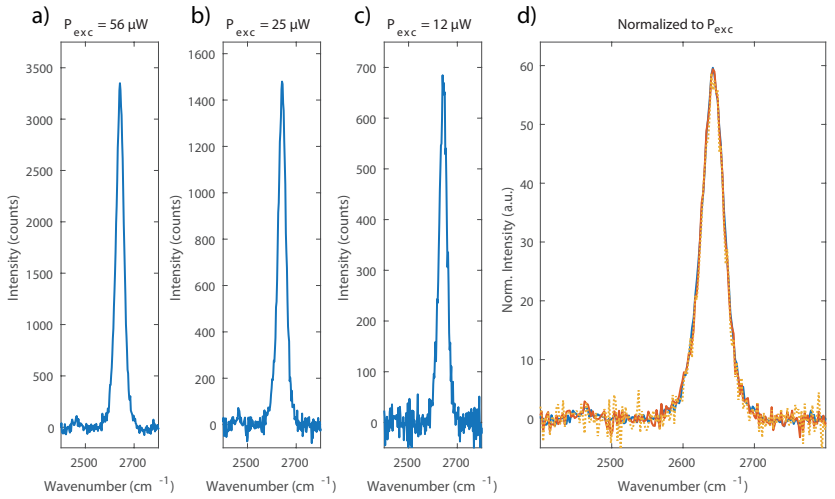

Figure S8: (a),(b) and (c) show the background corrected Raman 2D band recorded for cw excitation for three different excitation powers at 633 nm. (d) shows the comparison for all four measurements after normalization with the excitation power. The measurement with the lowest intensity is shown as dashed line for better readability.

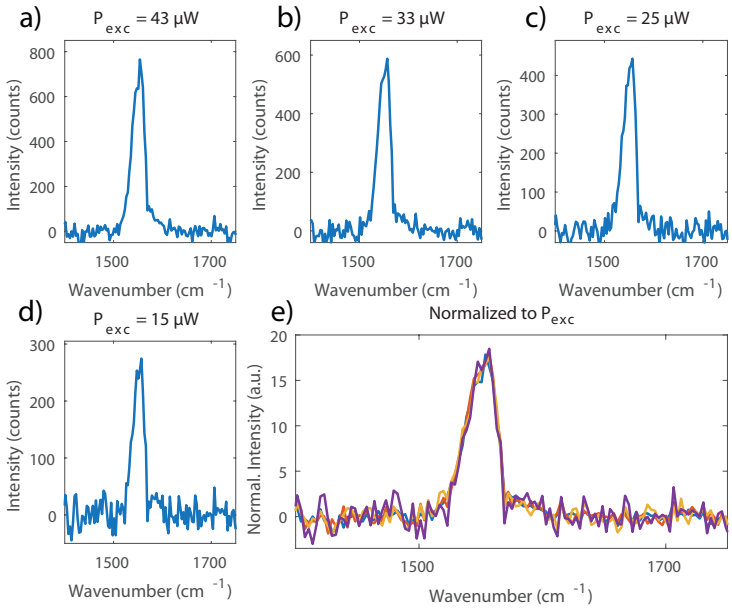

Figure S9: Raman spectra for different cw excitation intensities: (a),(b),(c) and (d) show the background corrected Raman G band recorded for cw excitation for four different excitation powers at $594\,\mathrm{nm}$. (e) shows the comparison for all four measurements after normalization with the excitation power.

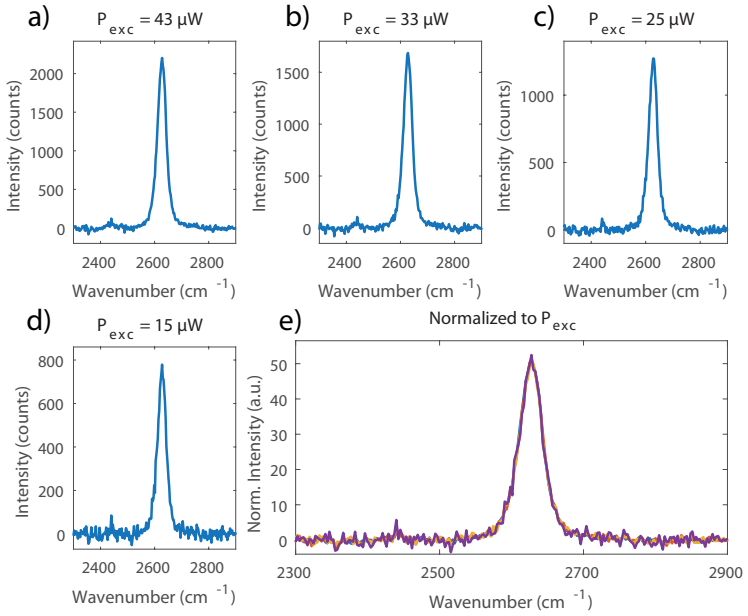

Figure S10: Raman spectra for different cw excitation intensities: (a),(b), (c) and (d) show the background corrected Raman 2D band recorded for cw excitation for four different excitation powers at $594\,\mathrm{nm}$. (e) shows the comparison for all four measurements after normalization with the excitation power.

4. Thermal emission from Graphene

4.1. Two temperature model (TTM) for thermal emission

The TTM which we use is almost identical to the model presented by Lui. et al.[2] It is based on the following two coupled ordinary differential equations:

$$\begin{aligned} \frac{dT_{el}(t)}{dt} &= \frac{I_{laser}(t) - \Gamma(T_{el}, T_{op})}{c_{el}(T_{el})}, \\ \frac{dT_{op}(t)}{dt} &= \frac{\Gamma(T_{el}, T_{op})}{c_{op}(T_{op})} - \frac{T_{op}(t) - T_0}{\tau_{op}}. \end{aligned} \tag{1}$$

They describe the temporal evolution of the electronic temperature T_{el} and the temperature of strongly coupled optical phonons (SCOP) T_{op}. The absorbed, time dependent laser irradiance is $I_{laser}(t)$ and given by the incoming laser pulse.

The time dependent irradiance was modelled as a squared hyperbolic secant (sech) function with a pulse duration of $600\,\mathrm{fs}$, multiplied by the fluence F. To account for the spatial inhomogeneous power distribution in the focus, F was not calculated as a overall average but for radial segments of the focus. The intensity distribution was modelled with a two dimensional Gaussian function with a full width half maximum of $350\,\mathrm{nm}$. Due to the reduced but unknown transmission of the used objective and the alternated absorption of graphene under high irradiation angles a reduction factor of $0.6(+-1)$ was introduced to the excitation power.

c_{el} and c_{op} are the specific heat capacities of the electrons and optical phonons, which both depend on the respective temperatures. τ_{op} is the decay time of the SCOPs which couple to a bath of other phonons. We used $\tau_{op} = 1.5\,\mathrm{ps}$ which is the same value used by Lui et al. in.[2] Γ is the electron-SCOP energy exchange rate and depends on both temperatures (see below). The specific heat of the electrons per unit area comes from the linear bands:

$$c_{el}(T_{el}) = \frac{18 \cdot \zeta(3)}{\pi \cdot (\hbar v_F)^2} \cdot k_B^3 \cdot T_{el}^2, \tag{2}$$

where $\zeta(3) = 1.202$ is the zeta function, $v_F = 1.1\,\mathrm{nm/fs}$ is the Fermi velocity of electrons in

graphene, and k_B is the Boltzmann constant. The phonon heat capacity of SCOPs in graphene at 200 meV can be estimated by:[2]

$$c_{op} = -4.79 \times 10^9 + 1.82 \times 10^7 \times T_{op} + 1.34 \times 10^4 \times T_{op}^2 + 5.16 \times T_{op}^3 \tag{3}$$

as given in $\mathrm{eV/cm^2/K}$. The exchange rate of electrons and SCOPs near the K-point is given by the following expression:[2]

$$\Gamma(T_{el}, T_{op}) = \beta \cdot \Big(\big(1 + n(T_{op})\big) \int D(E) \cdot D(E - \hbar\Omega) \cdot f(E, T_{el}) \cdot \big(1 - f(E - \hbar\Omega, T_{el})\big) dE \\ - n(T_{op}) \int D(E) \cdot D(E + \hbar\Omega) \cdot f(E, T_{el}) \cdot \big(1 - f(E + \hbar\Omega, T_{el})\big) dE \Big). \tag{4}$$

$\beta = 5e - 4\,\mathrm{eV^2cm^2/s}$ quantifies the overall SCOP-electron coupling strength. $\hbar\Omega = 200\,\mathrm{meV}$ is the energy of the SCOPs which is the amount of energy lost in every scattering event. The first term of the equation describes the emission and the second the absorption of a phonon. The density of states of electrons in graphene is given by:

$$D(E) = \begin{cases} \frac{2|E|}{\pi\hbar^2 v_F^2} & \text{for } E > 0, \\ 0 & \text{otherwise.} \end{cases} \tag{5}$$

The population of SCOPs at a temperature T_{op} is defined by the Bose-Einstein distribution: $n(T_{op}) = \left[\exp\left(\hbar\Omega / kT_{op}\right) - 1\right]^{-1}$, and the population of electrons is given by the Fermi-Dirac distribution, including the chemical potential of the electrons: $f(E, T_{el}) = \left[\exp\left((E - \mu)/kT_{el}\right) + 1\right]^{-1}$.

The solution of eq. 1 yields the time dependent electronic and phononic temperatures and has to be found by numerical integration. The assumption is that the observed photoluminescence can be described by black body radiation of the hot electrons. Their radiation losses on the other hand are so small that they do not need to be considered as decay channel in the TTM. The NLPL fluence

is then given by:[2]

$$I_{NLPL}(\omega) = \hbar \cdot \frac{\omega^3}{2\pi^2 c^2} \int \left[\exp\left(\frac{\hbar\omega}{kT_{el}(t)}\right) - 1 \right]^{-1} dt. \tag{6}$$

An example for the calculated electronic and SCOP temperatures using the two-temperature model is shown in S11 for an excitation intensity of 130 μW.

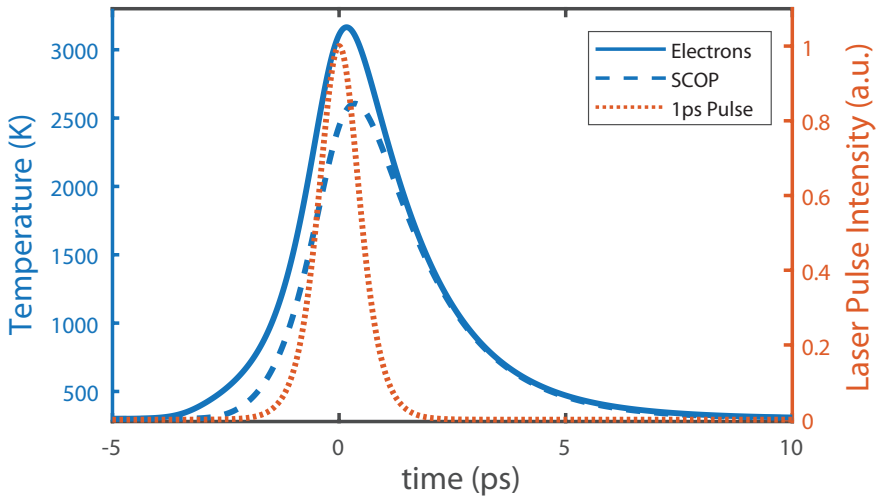

Figure S11: Example of time-dependent temperatures extracted from the two-temperature model. All calculations used a sech^2-pulse with a duration of 600 fs (equal to 1 ps FWHM) and the excitation powers were chosen according to the experiment. For the shown example the highest excitation power used in the measurements was chosen (130 μW). The temporal shape of the excitation pulse is shown as dotted line. The derived electronic temperatures are shown as solid line and the SCOP temperatures as dashed line, respectively.

4.2. Comparison of calculated and experimental recorded thermal emission

The calculated temperatures applying the two temperature model introduced above were verified by comparison with experimental thermal emission spectra from graphene. For six excitation powers ranging from 63 μW to 19 μW spectra were recorded and compared with the calculated emission spectra. Only a common scaling factor for all spectra was used to account for the absolute detection efficiency of the setup. In figure S12 a) the experimental spectra for excitation powers of 63 μW (black circles) and 48 μW (black crosses) together with the corresponding calcu-

lated thermal emission spectra (red dashed lines) are shown as examples. Figure S13 (see below) displays the recorded and calculated thermal emission in detail for all six excitation powers. The calculated maximum electron temperatures for all six excitation powers are given in figure S12 b).

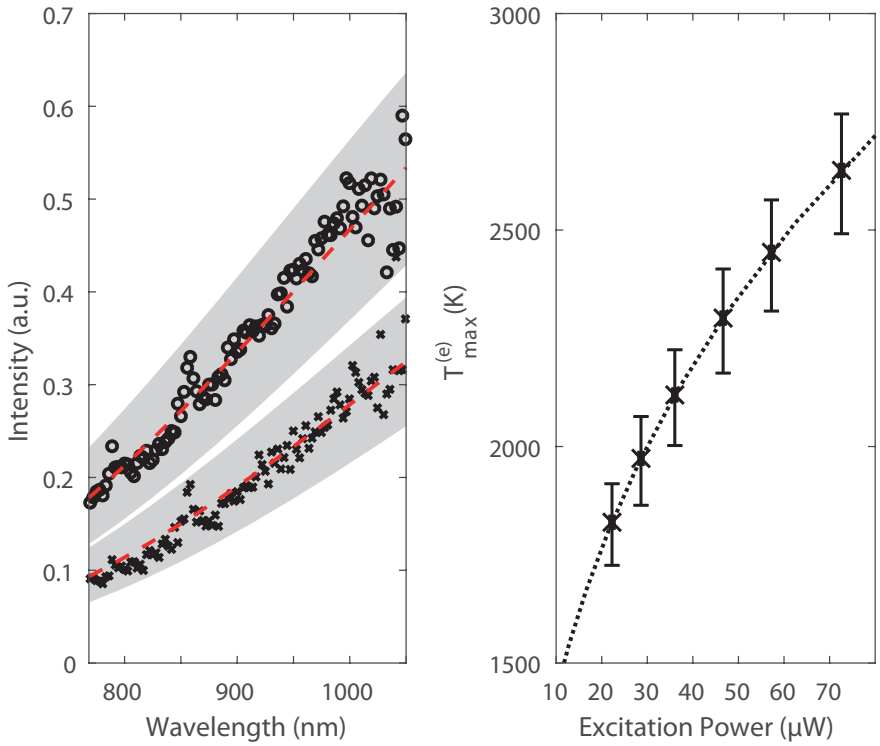

Figure S12: (a) Recorded thermal emission spectra for $63\,\mu$W (black circles) and $48\,\mu$W (black crosses) and the corresponding calculated thermal emission using the TTM (red dashed lines). The peak at 857 nm is due to weak emission from the glass substrate. (b) Calculated maximum electron temperature for all six excitation powers (black crosses). The black dashed line represents the correlation between maximum electron temperature and excitation power.

The recorded spectra match the calculated thermal emission well verifying the applicability of the model in our experiment and the comparability of the calculation and the experiment.

4.3. Thermal emission at $2\omega_L$

An alternative mechanism for the optical absorption and emission of graphene was proposed by Heller and co-authors[3] as mentioned in the main manuscript. Hereafter, absorption and broadband emission are attributed to a manifold of indirect optical transitions connecting a broad range of

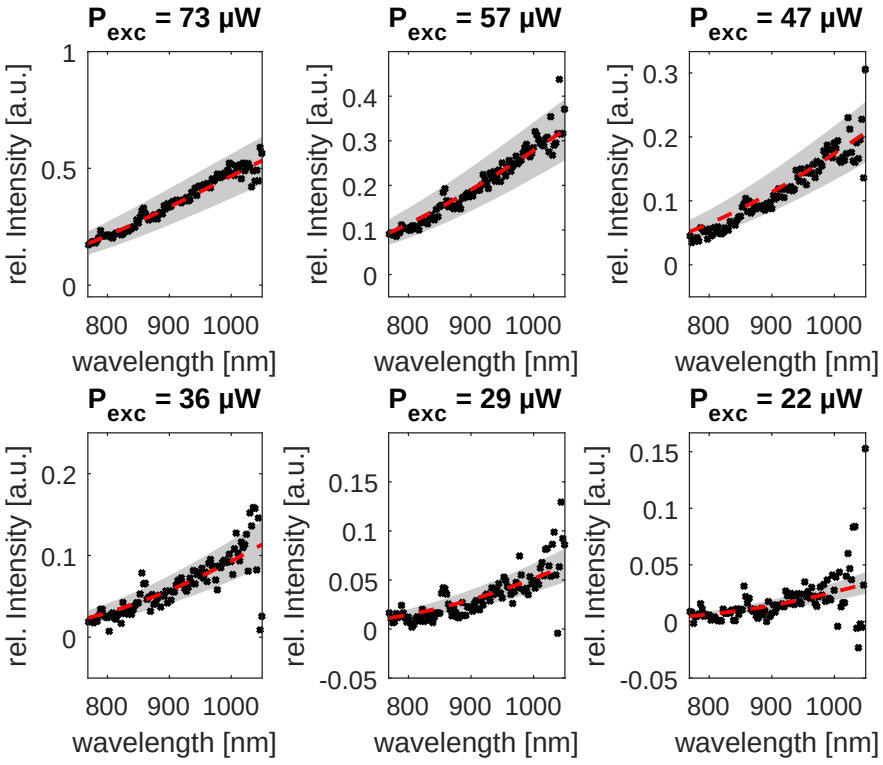

Figure S13: Comparison between recorded (black crosses) and calculated thermal emission spectra (dashed red line) from graphene for six different excitation powers. The spectra were spectra calculated using the TTM as described in the text. A single amplitude scaling factor was applied to all experimental curves to account for the detection sensitivity of the setup.

k-states. A key prediction of the underlying model is that broadband emission from graphene is limited to a maximum energy of twice the excitation energy ($2\omega_L$).[3]

To test this prediction, we studied graphene's broadband emission using near-infrared pulsed laser excitation provided by a Ti:Sa-oscillator with a pulse length of about $200\,\mathrm{fs}$ and a central wavelength of $920\,\mathrm{nm}$. The excitation laser light was suppressed using appropriate shortpass filters. The recorded spectrum was calibrated by the spectral sensitivity profile of the detection system. The recorded spectrum, shown in figure S14, clearly extends beyond $2\omega_L$. In addition, no step or sudden change in intensity is observed at twice the excitation energy corresponding to $460\,\mathrm{nm}$. This is in agreement with the thermal emission spectra reported by Liu et al.[2]

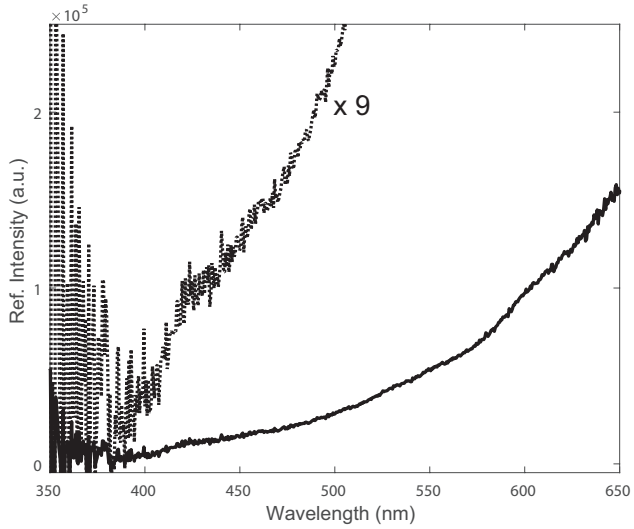

Figure S14: Broadband emission from graphene detected upon pulsed laser excitation at $920\,\mathrm{nm}$. The emission is seen to extend below 460 nm with a smoothly decreasing intensity profile.

References

(1) Romagnoli, M.; Sorianello, V.; Midrio, M.; Koppens, F. H. L.; Huyghebaert, C.; Neumaier, D.; Galli, P.; Templ, W.; D'Errico, A.; Ferrari, C. F. *Nat. Rev. Mater.* **2018**, *3*, 392–414.

(2) Lui, C. H.; Mak, K. F.; Shan, J.; Heinz, T. F. *Phys. Rev. Lett.* **2010**, *105*, 127404.

(3) Yang, Y.; Kolesov, G.; Kocia, L.; Heller, E. J. *Nano Lett.* **2017**, *17*, 6077–6082.